Magn Reson Med Sci 2019; 18; 194–199
doi:10.2463/mrms.mp.2018-0043
Published Online: November 9, 2018

MAJOR PAPER

Signal Intensity of the Cerebrospinal Fluid after Intravenous Administration of Gadolinium-based Contrast Agents: Strong Contrast Enhancement around the Vein of Labbe

Toshio Ohashi[1*], Shinji Naganawa[2], Eriko Ogawa[1], Toshio Katagiri[1], and Kayao Kuno[3]

Purpose: Since the first report on the deposition of gadolinium in the brain parenchyma after repeated intravenous administrations of gadolinium-based contrast agent GBCA (IV-GBCA), the mechanisms of penetration and retention are still remaining a hot topic of discussion and a target of investigation. We routinely obtain endolymphatic hydrops (EH) images at 4 h after IV administration of a single dose (SD) of GBCA (IV-SD-GBCA) using heavily T_2-weighted three-dimensional fluid-attenuated inversion recovery imaging (hT_2W-3D-FLAIR). Occasionally, we have encountered cases, which indicate high-signal intensity (SI) in the cerebrospinal fluid (CSF) surrounding the vein of Labbe. The purpose of the present study was to investigate the degree of contrast enhancement of the CSF surrounding the vein of Labbe on hT_2W-3D-FLAIR after IV-SD-GBCA in comparison with other CSF spaces.

Materials and Methods: In 25 patients with a suspicion of EH, a magnetic resonance cisternography (MRC) and an hT_2W-3D-FLAIR were obtained at 4 h after IV-SD-GBCA. The perivascular space (PVS) in the basal ganglia, CSF spaces in the ambient cistern (CSF-Amb), the CSF surrounding the superficial middle cerebral vein (CSF-SMCV), and the CSF surrounding the vein of Labbe (CSF-VL) were segmented on MRC. The PVS and CSF regions were co-registered onto the hT_2W-3D-FLAIR and the SI of the PVS and CSF spaces were measured. The SI ratio (SIR) of the post-contrast hT_2W-3D-FLAIR to the pre-contrast hT_2W-3D-FLAIR was measured. Significant differences were evaluated using Steel-Dwass's test for multiple comparisons.

Results: The SIR of the CSF-VL was significantly higher than that of the PVS ($P = 0.008$), the CSF-Amb ($P = 0.021$), and the CSF-SMCV ($P = 0.023$).

Conclusion: The strong contrast enhancement of CSF space around the vein of Labbe was confirmed on hT_2W-3D-FLAIR at 4 h after IV-GBCA compared to the PVS and the other CSF spaces.

Keywords: *cerebrospinal fluid, gadolinium, glymphatic system, magnetic resonance imaging, vein*

Introduction

Previously, it was believed that gadolinium-based contrast agents (GBCAs) with an intact chelate did not pass the brain–blood barrier (BBB) and penetrate into the brain parenchyma directly.[1] Therefore, MRI using GBCAs has been performed routinely to reveal lesions with a disrupted BBB, such as tumors, infections, and metastases.

Since the first report on gadolinium deposition in brain regions, such as the dentate nucleus and globus pallidus after repeated intravenous administrations of GBCA (IV-GBCA), the mechanisms of penetration and retention are still remaining a hot topic of discussion and a target of investigation.[2] Recently, a hypothesis for waste clearance system in the brain through a cerebrospinal fluid (CSF)—interstitial fluid pathway through perivascular space (PVS) has been proposed and named as "glymphatic system."[3] While, leakage of GBCAs into the PVS and CSF that comprises the glymphatic system was reported on heavily T_2-weighted three-dimensional fluid-attenuated inversion recovery images (hT_2W-3D-FLAIR) in a delayed phase after IV-GBCA in human subjects without renal insufficiency.[4,5]

[1]Department of Radiology, Kamiiida Daiichi General Hospital, 2-70 Kamiiida-kitamachi, Kita-ku, Nagoya, Aichi 462-0802, Japan
[2]Department of Radiology, Nagoya University Graduate School of Medicine, Aichi, Japan
[3]Department of Otorhinolaryngology, Kamiiida Daiichi General Hospital, Aichi, Japan
*Corresponding author, E-mail: t.ohashi@re.commufa.jp

Received: March 13, 2018 | Accepted: September 7, 2018

Therefore, it is presumed that GBCA penetration into the CSF may be linked to glymphatic function.[5] However, the pathway for IV-GBCA leakage into the CSF space has not been clarified. Although the choroid plexus, which has been regarded as the place of CSF secretion through the CSF-BBB, seemed to be a candidate for this leakage pathway, there is a recent report suggesting that choroid plexus function is insufficient to regulate CSF circulation, formation, absorption, and pressure.[6,7]

The FLAIR sequence is sensitive to GBCA distribution in fluid compared with conventional T_1-weighted imaging (T_1WI).[8] Especially, the hT_2W-3D-FLAIR sequence has very high sensitivity to subtle T_1 shortening in the fluid, such as GBCA at low concentrations within CSF.[9] This imaging sequence has enabled the detection of slight amounts of GBCA in the perilymph space after IV administration of a single dose (IV-SD-GBCA), and a method to visualize endolymphatic hydrops (EH) by clinical MRI has been developed.[10,11] We routinely obtain EH images at 4 h after IV-SD-GBCA using hT_2W-3D-FLAIR and evaluate the volume of EH quantitatively in accordance with our previously reported studies.[12–15] We have occasionally encountered cases with high-signal intensity (SI) in the CSF surrounding the vein of Labbe, also known as the inferior anastomotic vein. Therefore, we hypothesized that an assessment of the strong contrast enhancement might be helpful to elucidate the mechanism of GBCA leakage into the CSF.

The purpose of the present study was to investigate the degree of contrast enhancement on hT_2W-3D-FLAIR of the CSF surrounding the vein of Labbe compared to different CSF-containing regions after IV-SD-GBCA.

Materials and Methods

Patients

Twenty-five patients (11 men, 14 women; ages: 27–74 years, median 55 years) who underwent MR examination from October 2015 to January 2018 to assess clinically suspected EH were enrolled. We confirmed that there had been no significant misregistration in all patients by observing inner ear structure on a subtraction image of MR cisternography (MRC) from hT_2W-3D-FLAIR: HYbriD of reversed image of MR cisternography and positive perilymph signal (HYDROPS2).[16] The estimated glomerular filtration rate (eGFR) of all patients exceeded 60 mL/min/1.73 m^2. The medical ethics committee of our hospital approved this retrospective study and waived informed consent.

MR imaging

All imaging was performed on a 3T MR scanner (MAGNETOM Skyra, Siemens Healthcare, Erlangen, Germany) with a 32 channel-phased array head coil. MR examinations were performed before and 4 hours after IV-SD-GBCA (0.1 mmol/kg body weight) to evaluate the degree of EH. For the GBCA, a macrocyclic agent, gadoteridol (Gd-HP-DO3A; ProHance, Eisai, Tokyo, Japan), was administered. The patients underwent an MRC and an hT_2W-3D-FLAIR sequence, according to a previously reported protocol used for the evaluation of EH.[12–15] For the MRC, a heavily T_2W 3D-turbo spin echo sequence (TR = 4400 ms, TE = 544 ms) with a variable refocusing flip angle was used. The hT_2W-3D-FLAIR was a similar sequence type to the MRC; however, a non-selective inversion recovery pulse and extended TR were applied in this sequence (TR = 9000 ms, TE = 544 ms, TI = 2250 ms). The resolution parameters and the range of imaging axial slabs were aligned in both sequences. The voxel size was 0.5 × 0.5 × 1.0 mm^3. The slab thickness was 104 mm. The oblique degree of imaging slab was parallel to the anterior commissure (AC)–posterior commissure (PC) line and bilateral internal auditory canal in the axial section, and the center was set at the level of internal auditory canal. The details of the imaging parameters are indicated in Table 1.

Image analysis

Two radiological technologists with 8 and 15 years of experience in MRI evaluated the images using OsiriX (version 5.8

Table 1 Pulse sequence parameters

Parameter	MR cisternography	Heavily T_2-weighted 3D-FLAIR
Sequence type	SPACE with restore pulse	SPACE with inversion pulse
TR (ms)	4400	9000
TE (ms)	544	544
Inversion time (ms)	NA	2250
Fat suppression	CHESS	CHESS
Flip angle (degree)	90/initial 180 decrease to constant 120	90/initial 180 decrease to constant 120
Section thickness/ Gap (mm)	1.0/0.0	1.0/0.0
Pixel size (mm)	0.5 × 0.5	0.5 × 0.5
Number of slices	104	104
Echo train length	173	173
Field of view (mm)	165 × 196	165 × 196
Matrix size	324 × 384	324 × 384
Parallel imaging/ Acceleration factor	GRAPPA/2	GRAPPA/2
Band width (Hz/Px)	434	434
Number of excitations	1.8	4
Scan time (min)	3.4	15.2

FLAIR, fluid-attenuated inversion recovery; SPACE, sampling perfection with application-optimized contrasts using different flip angle evolutions; NA, not applicable; CHESS, chemical shift selective; GRAPPA, generalized auto- calibrating partially parallel acquisition.

32 bit, Pixmeo SARL Bernex, Switzerland, http://www.osirix-viewer.com/). The SI of the PVS in the basal ganglia, the CSF in the ambient cistern (CSF-Amb), the CSF surrounding the superficial middle cerebral vein (CSF-SMCV), and the CSF surrounding the vein of Labbe (CSF-VL) were used for the measurements.

First, the PVS in the bilateral basal ganglia was segmented on the middle slice of the MRC that contained both the AC and PC using a region growing function of OsiriX. The region growing function allows to segment the voxels that fulfill the user-defined threshold range. The PVS was regarded as an isolated area that indicates fluid signal in the basal ganglia on the MRC. The SI threshold of the region growing method was set to the half value of the SI that the CSF in the Sylvian fissure indicated. Then, the PVS region on the MRC was co-registered by copy and paste onto the hT_2W-3D-FLAIR, and the SI of the PVS on hT_2W-3D-FLAIR was measured. An example of the PVS segmentation is indicated in Fig. 1.

In the next step, the CSF regions were segmented. Circular ROIs with a 6 mm diameter were set bilaterally in the ambient cistern, the SMCV, and the VL. The ROI in the SMCV was drawn in the vessel-formed structure showing a flow void in the anterior superficial part of the temporal lobe on the MRC. The ROI in the VL was placed in the most posterior located vessel-formed structure showing a flow void in the middle or posterior superficial part of the temporal lobe on the MRC. To exclude the vessels, bones, or brain parenchyma from the ROIs, the CSF regions within the ROIs were segmented using the region growing method. The half value of the SI that the CSF in the Sylvian fissure indicated was applied for the SI threshold of the region growing method. The CSF regions on the MRC were co-registered by copy and paste onto the hT_2W-3D-FLAIR, and the SI of the CSF-Amb, CSF-SMCV, and CSF-VL on hT_2W-3D-FLAIR were measured. An example of the CSF segmentation is indicated in Fig. 2.

The SI measurements were performed on both the pre- and post-contrast hT_2W-3D-FLAIR.

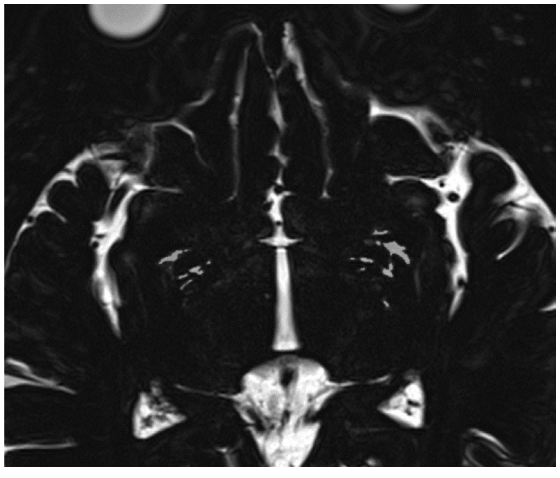

Fig. 1 An example of segmentation of the perivascular space (PVS) in the basal ganglia for the signal intensity measurement. The PVS region was segmented using a region-growing method on the magnetic resonance cisternography.

Statistical analysis

The statistical analyses were performed with R software (version 3.4.3, The R Foundation, https://www.R-project.org/) using the mean value of the two observers' measurements and the bilateral values were averaged. We defined the ratio of the SI on the post-contrast hT_2W-3D-FLAIR to the SI of the pre-contrast hT_2W-3D-FLAIR as the SI ratio (SIR): SIR = SI of the post-contrast hT_2W-3D-FLAIR/SI of the pre-contrast hT_2W-3D-FLAIR. The significant differences between the SIR of the PVS, CSF-Amb, CSF-SMCV, and CSF-VL were evaluated using Steel-Dwass's test for multiple comparisons. We considered a P value less than 0.05 as statistically significant. The intra-class correlation coefficient between the two observers' measurements was also calculated.

Results

The SIR of the CSF-VL was significantly higher than that of the PVS (P = 0.008), the CSF-Amb (P = 0.021), and the CSF-SMCV (P = 0.023). Figure 3 shows the comparison of the SIR of the PVS and the CSF spaces. The representative images obtained in the present study are indicated in Fig. 4.

The intra-class correlation coefficient between the SIR measurements from the two observers' was 0.835 for the PVS, 0.673 for the CSF-Amb, 0.743 for the CSF-SMCV, and 0.929 for the CSF-VL.

Discussion

In the present study, the SIR of the PVS and the CSF spaces were investigated using hT_2W-3D-FLAIR prior to and at 4 h after IV-SD-GBCA. The SIR of the CSF-VL was significantly higher than that of the PVS and the other CSF spaces. The strong enhancement of the CSF space around the VL indicates GBCA penetration and suggests that the VL might be a pathway by which intravenously administered GBCA leaks into the CSF spaces. GBCA penetration into the CSF has been regarded as a result of increased BBB permeability.[17] Based on this concept, MR diagnostic findings for CSF signal alteration such as "hyperintense acute reperfusion marker" has been described as a sign for early BBB disruption in acute ischemic stroke.[18] A recent study using a conventional 3D-FLAIR sequence at 16 min after IV-SD-GBCA confirmed contrast enhancement of the CSF surrounding cortex in 21 out (28%) of 74 subjects.[19] They suggested that the signal enhancement of pericortical CSF was associated with increasing age, and that was a result in BBB disruption, which was caused by

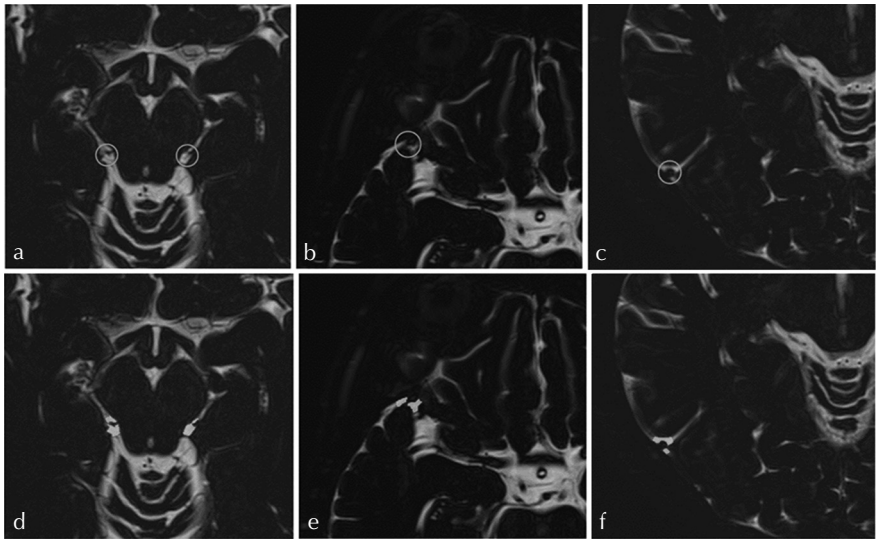

Fig. 2 An example of segmentation of the cerebrospinal fluid (CSF) spaces for the signal intensity measurement. Circular ROIs with a 6 mm diameter were placed in the ambient cistern (**a**), the superficial middle cerebral vein (SMCV) (**b**), and vein of Labbe (**c**) on the magnetic resonance cisternography. To exclude the vessels, bones, or brain parenchyma from the ROIs, the CSF regions within the ROIs in the ambient cistern (**d**), surrounding SMCV (**e**), and surrounding the vein of Labbe (**f**) were segmented using the region growing method.

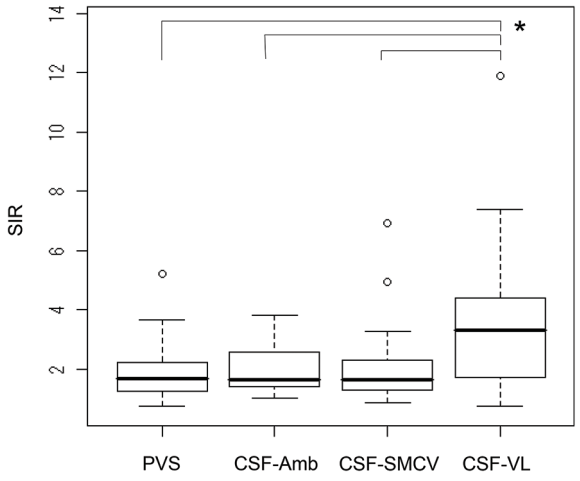

Fig. 3 A comparison of the signal intensity ratio (SIR) of the perivascular space (PVS) in the basal ganglia and the cerebrospinal fluid (CSF) spaces. An asterisk indicates the statistically significant difference. The SIR of the CSF surrounding the vein of Labbe (CSF-VL) was increased significantly compared to that of the PVS, the CSF in the ambient cistern (CSF-Amb), and the CSF surrounding the superficial middle cerebral vein (CSF-SMCV).

cerebral ischemia or hypoxia.[19] In the present study, the oldest male subject indicated especially strong enhancement of CSF surrounding SMCV and the VL, the outliers on Fig. 3. The leakage of GBCA might be related to the aging process. However, the subjects in the present study did not have a history of cerebrovascular disease that could cause BBB disruption. The hT_2W-3D-FLAIR sequence has a higher sensitivity for small amounts of GBCA diluted in fluid than the conventional FLAIR sequence used in the previous study.[9,19] The waiting time after IV-SD-GBCA was much longer in the present study. In addition, according to a previous study on healthy human subjects using the hT_2W-3D-FLAIR sequence, the enhancement of the CSF was confirmed at 1.5 h after IV-SD-GBCA and the signal increase persisted for at least 6 h.[4,5] The GBCA leakage was observed not only in subjects with pathologically disrupted BBB, but also in subjects with presumed intact BBB. Studies on rats also indicate prompt leakage of GBCA to CSF after IV administration.[20,21] Therefore, these findings suggest that there might be two mechanisms for GBCA penetration into the CSF space from the blood; one is "fast and thick," which is a result of a disrupted BBB, and the other is "slow and slight," which is seen in subjects with an intact BBB.

There are several studies in which CSF enhancement after IV-SD-GBCA has been reported. One previously reported study confirmed a strong enhancement of the CSF spaces around the peripheral part of cerebral nerves such as the optic, trigeminal, and vestibulocochlear nerves, compared with the ambient cistern on hT_2W-3D-FLAIR at a delayed phase after IV-SD-GBCA.[4] The leakage of GBCA in the PVS, which is the key organ for the glymphatic system, after IV-SD-GBCA was reported.[5] In a recent study, enhancement around the organum vasculosum of the lamina terminalis, a circumventricular organ which lacks a BBB, was observed after IV-SD-GBCA using hT_2W-3D-FLAIR.[22] Therefore, it is possible that these regions, including the VL, might play a role in the leakage of GBCA into the CSF from the blood, acting as a part of the glymphatic system pathway.

The glymphatic system is speculated to be responsible for homeostasis of the CSF. Dysfunction of the glymphatic system causes an accumulation of toxic solutes including amyloid β, which is a risk factor for the development of Alzheimer's disease.[3] Recent clinical imaging using hT_2W-3D-FLAIR showed that the large PVS did not enhance at 4 h after IV-SD-GBCA; however, moderate sized PVS was enhanced.[23] An enlarged PVS is a feature of cerebral small vessel diseases, and a recent review proposed an association between cerebral small vessel diseases and glymphatic dysfunction.[24] In addition, a strong negative correlation between enhancement of the PVS in the basal ganglia and the volume of the EH, as well as

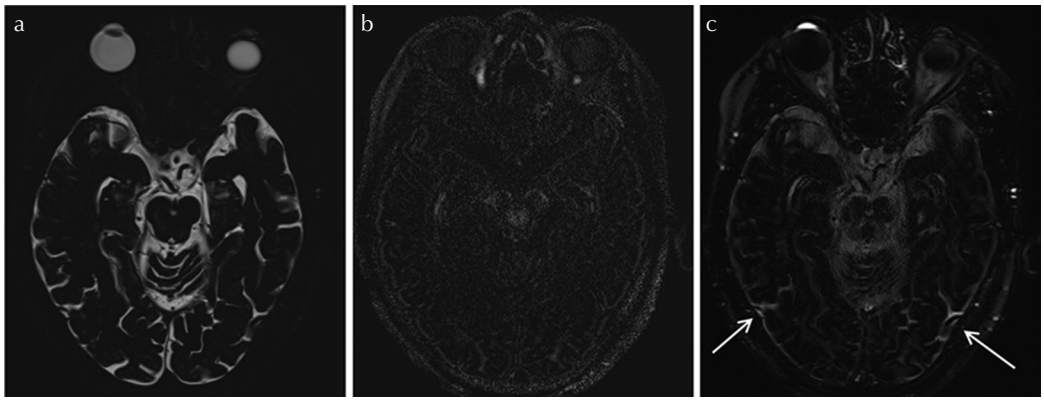

Fig. 4 A representative image: a 56-year-old woman with clinical suspicion of endolymphatic hydrops. (**a**) A magnetic resonance cisternography as anatomical reference for the fluid space. (**b**) A heavily T_2-weighted 3D fluid-attenuated inversion recovery image (hT_2W-3D-FLAIR) obtained before administration of the contrast agent. (**c**) A hT_2W-3D-FLAIR obtained at 4 h after administration of the contrast agent. The cerebrospinal fluid (CSF) surrounding the vein of Labbe indicates higher signal intensity than the other CSF spaces (arrows).

a positive correlation between enhancement of the PVS and that of the ambient cistern was reported in a previous study.[25] The leakage of GBCA in the brain might depend on the state of glymphatic function. A further study correlating the degree of enhancement of the CSF space around the VL and patients' symptoms as a result of the glymphatic dysfunction is warranted to further our understanding of the glymphatic system.

The present study has several limitations. Although we assessed the patients' misregistration using HYDROPS2 images[16] and confirmed that there had been no significant misregistration in all patients, there might be very small patients' movement that affects the measurements of SI in some cases. The results in the present study may include some bias, because all the subjects in the present study were suspected to be EH, the volume of which was correlated with the enhancement of PVS in the basal ganglia.[25] Furthermore, in a few cases, CSF surrounding SMCV indicated strong enhancement. There might be a possibility that not only the vein of Labbe but also other superficial cerebral vein is the pathway where GBCA leaks into the CSF space. However, the cranial edge of the scanning range was the level of the lateral ventricle in the present study. Therefore, the further study including the whole brain on the healthy human subjects should be investigated.

Conclusion

The strong contrast enhancement of the CSF space around the vein of Labbe was confirmed on hT_2W-3D-FLAIR at 4 h after IV-GBCA compared with the PVS and the other CSF spaces.

The vein of Labbe might be involved in the process of GBCA leakage into the CSF.

Conflicts of Interest

All authors do not have any conflicts of interest regarding the present study.

References

1. Weinmann HJ, Brasch RC, Press WR, Wesbey GE. Characteristics of gadolinium-DTPA complex: a potential NMR contrast agent. AJR Am J Roentgenol 1984; 142: 619–624.
2. Taoka T, Naganawa S. Gadolinium-based contrast media, cerebrospinal fluid and the glymphatic system: possible mechanisms for the deposition of gadolinium in the brain. Magn Reson Med Sci 2018;17:111–119.
3. Iliff JJ, Wang M, Liao Y, et al. A paravascular pathway facilitates CSF flow through the brain parenchyma and the clearance of interstitial solutes, including amyloid β. Sci Transl Med 2012; 4:147ra111.
4. Naganawa S, Suzuki K, Yamazaki M, Sakurai Y. Serial scans in healthy volunteers following intravenous administration of gadoteridol: time course of contrast enhancement in various cranial fluid spaces. Magn Reson Med Sci 2014; 13:7–13.
5. Naganawa S, Nakane T, Kawai H, Taoka T. Gd-based contrast enhancement of the perivascular spaces in the basal ganglia. Magn Reson Med Sci 2017; 16:61–65.
6. Orešković D, Radoš M, Klarica M. Cerebrospinal fluid secretion by the choroid plexus? Physiol Rev 2016; 96:1661–1662.
7. Orešković D, Radoš M, Klarica M. Role of choroid plexus in cerebrospinal fluid hydrodynamics. Neuroscience 2017; 354:69–87.
8. Fukuoka H, Hirai T, Okuda T, et al. Comparison of the added value of contrast-enhanced 3D fluid-attenuated inversion recovery and magnetization-prepared rapid acquisition of gradient echo sequences in relation to conventional postcontrast T_1-weighted images for the evaluation of leptomeningeal diseases at 3T. AJNR Am J Neuroradiol 2010; 31:868–873.
9. Naganawa S, Kawai H, Sone M, Nakashima T. Increased sensitivity to low concentration gadolinium contrast by optimized heavily T_2-weighted 3D-FLAIR to visualize endolymphatic space. Magn Reson Med Sci 2010; 9:73–80.

10. Naganawa S, Yamazaki M, Kawai H, Bokura K, Sone M, Nakashima T. Visualization of endolymphatic hydrops in Ménière's disease with single-dose intravenous gadolinium-based contrast media using heavily T_2-weighted 3D-FLAIR. Magn Reson Med Sci 2010; 9:237–242.
11. Nakashima T, Pyykkö I, Arroll MA, et al. Meniere's disease. Nat Rev Dis Primers 2016; 2:16028.
12. Nakashima T, Naganawa S, Pyykkö I, et al. Grading of endolymphatic hydrops using magnetic resonance imaging. Acta Otolaryngol Suppl 2009; 560:5–8
13. Naganawa S, Nakashima T. Visualization of endolymphatic hydrops with MR imaging in patients with Ménière's disease and related pathologies: current status of its methods and clinical significance. Jpn J Radiol 2014; 32:191–204.
14. Naganawa S, Ohashi T, Kanou M, Kuno K, Sone M, Ikeda M. Volume quantification of endolymph after intravenous administration of a single dose of gadolinium contrast agent: comparison of 18- versus 8-minute imaging protocols. Magn Reson Med Sci 2015; 14:257–262.
15. Naganawa S. The technical and clinical features of 3D-FLAIR in neuroimaging. Magn Reson Med Sci 2015; 14:93–106.
16. Naganawa S, Yamazaki M, Kawai H, Bokura K, Sone M, Nakashima T. Imaging of Ménière's disease by subtraction of MR cisternography from positive perilymph image. Magn Reson Med Sci 2012; 11:303–309.
17. Warach S, Latour LL. Evidence of reperfusion injury, exacerbated by thrombolytic therapy, in human focal brain ischemia using a novel imaging marker of early blood-brain barrier disruption. Stroke 2004; 35:2659–2661.
18. Köhrmann M, Struffert T, Frenzel T, Schwab S, Doerfler A. The hyperintense acute reperfusion marker on fluid-attenuated inversion recovery magnetic resonance imaging is caused by gadolinium in the cerebrospinal fluid. Stroke 2012; 43:259–261.
19. Freeze WM, Schnerr RS, Palm WM, et al. pericortical enhancement on delayed postgadolinium fluid-attenuated inversion recovery images in normal aging, mild cognitive impairment, and alzheimer disease. AJNR Am J Neuroradiol 2017; 38:1742–1747.
20. Jost G, Frenzel T, Lohrke J, Lenhard DC, Naganawa S, Pietsch H. Penetration and distribution of gadolinium-based contrast agents into the cerebrospinal fluid in healthy rats: a potential pathway of entry into the brain tissue. Eur Radiol 2017; 27:2877–2885.
21. Taoka T, Jost G, Frenzel T, Naganawa S, Pietsch H. Impact of the glymphatic system on the kinetic and distribution of gadodiamide in the rat brain: observations by dynamic MRI and effect of circadian rhythm on tissue gadolinium concentrations. Invest Radiol 2018; 53:529–534.
22. Naganawa S, Taoka T, Kawai H, Yamazaki M, Suzuki K. Appearance of the organum vasculosum of the lamina terminalis on contrast-enhanced MR imaging. Magn Reson Med Sci 2018; 17:132–137.
23. Naganawa S, Nakane T, Kawai H, Taoka T. Lack of contrast enhancement in a giant perivascular space of the basal ganglion on delayed FLAIR images: implications for the glymphatic system. Magn Reson Med Sci 2017; 16:89–90.
24. Mestre H, Kostrikov S, Mehta RI, Nedergaard M. Perivascular spaces, glymphatic dysfunction, and small vessel disease. Clin Sci 2017; 131:2257–2274.
25. Ohashi T, Naganawa S, Katagiri T, Kuno K. Relationship between contrast enhancement of the perivascular space in the basal ganglia and endolymphatic volume ratio. Magn Reson Med Sci 2018; 17:67–72.